Inorg. Chem. **2007**, *46*, 11112–11121

DNA Cleavage by New Oxovanadium(IV) Complexes of *N*-Salicylidene α-Amino Acids and Phenanthroline Bases in the Photodynamic Therapy Window

Pijus K. Sasmal, Ashis K. Patra, Munirathinam Nethaji, and Akhil R. Chakravarty*

Department of Inorganic and Physical Chemistry, Indian Institute of Science, Bangalore 560012, India

Received June 16, 2007

Oxovanadium(IV) complexes [VO(salmet)(B)] (**1**–**3**) and [VO(saltrp)(B)] (**4**–**6**), where salmet and saltrp are *N*-salicylidene-L-methionate and *N*-salicylidene-L-tryptophanate, respectively, and B is a *N,N*-donor heterocyclic base (viz. 1,10-phenanthroline (phen, **1**, **4**), dipyrido[3,2-d:2′,3′-f]quinoxaline (dpq, **2**, **5**), and dipyrido[3,2-a:2′,3′-c]phenazine (dppz, **3**, **6**)) are prepared and characterized and their DNA binding and photoinduced DNA cleavage activity studied. Complexes **1**, **2**, and **4** are structurally characterized by single-crystal X-ray crystallography. The molecular structure shows the presence of a vanadyl group in the VO_3N_3 coordination geometry. The dianionic α-amino acid Schiff base acts as a tridentate *O,N,O*-donor ligand in a meridional binding mode. The *N,N*-donor heterocyclic base displays a chelating mode of bonding with a N-donor site trans to the oxo group. The complexes show a d–d band in the range of 680–710 nm in DMF with a shoulder near 840 nm. They exhibit an irreversible oxidative cyclic voltammetric response near 0.8 V assignable to the V(V)/V(IV) couple and a quasi-reversible V(IV)/V(III) redox couple near –1.1 V vs SCE in DMF–0.1 M TBAP. The complexes show good binding propensity to calf thymus DNA giving binding constant values in the range from 5.2×10^4 to 7.2×10^5 M^{-1}. The binding site size, thermal melting, and viscosity data suggest DNA surface and/or groove binding nature of the complexes. The complexes show poor "chemical nuclease" activity in the dark in the presence of 3-mercaptopropionic acid or hydrogen peroxide. The dpq and dppz complexes show efficient DNA cleavage activity on irradiation with UV-A light of 365 nm via a mechanistic pathway involving formation of singlet oxygen as the reactive species. They also show significant DNA cleavage activity on photoexcitation in red light (>750 nm) by $^1O_2$ species. Observation of red-light-induced cleavage of DNA is unprecedented in the vanadium chemistry. The DNA cleavage activity is metal promoted as the ligands or vanadyl sulfate alone are cleavage inactive on photoirradiation at these wavelengths.

Introduction

Photodynamic therapy (PDT) is an emerging method of noninvasive treatment of cancer with an advantage of having localized photoactivation of the drug at the targeted tumor cells, leaving the healthy cells unaffected from the phototoxicity of the PDT agent.[1−5] This method is superior in the sense that it eliminates the toxic and resistance effects of chemotherapeutic drugs like cis-platin and its derivatives.[6−8] Photofrin, which is a mixture of hematoporphyrins and its derivatives, is the FDA-approved PDT drug used for lung and esophageal cancers. Photoactivation of Photofrin at its

* To whom correspondence should be addressed. Fax: 91-80-23600683. E-mail: arc@ipc.iisc.ernet.in.

(1) Bonnet, R. *Chemical Aspects of Photodynamic Therapy*; Gordon & Breach: London, U.K., 2000.
(2) Wei, W.-H.; Wang, Z.; Mizuno, T.; Cortez, C.; Fu, L.; Sirisawad, M.; Naumovski, L.; Magda, D.; Sessler, J. L. *Dalton Trans.* **2006**, 1934.
(3) Henderson, B. W.; Busch, T. M.; Vaughan, L. A.; Frawley, N. P.; Babich, D.; Sosa, T. A.; Zollo, J. D.; Dee, A. S.; Cooper, M. T.; Bellnier, D. A.; Greco, W. R.; Oseroff, A. R. *Cancer Res.* **2000**, *60*, 525.
(4) Sternberg, E. D.; Dolphin, D.; Brückner, C. *Tetrahedron* **1998**, *54*, 4151.
(5) DeRosa, M. C.; Crutchley, R. J. *Coord. Chem. Rev.* **2002**, *233*−*234*, 351.
(6) (a) Barnes, K. R.; Lippard, S. J. *Met. Ions Biol. Syst.* **2004**, *42*, 143. (b) Reedijk, J. *Proc. Natl. Acad. Sci. U.S.A.* **2003**, *100*, 3611.
(7) Hartmann, J. T.; Lipp, H. P. *Expert Opin. Pharmacother.* **2003**, *4*, 889.
(8) Markman, M. *Expert Opin. Drug Saf.* **2003**, *2*, 597.

10.1021/ic7011793 CCC: $37.00
Published on Web 11/17/2007

lowest energy Q band of 630 nm generates a $^1\pi\pi^*$ state with subsequent formation of its triplet state $^3\pi\pi^*$ that activates molecular oxygen to form cytotoxic singlet oxygen ($^1O_2$) species.[9] Porphyrin-based drugs show dark toxicity and hepatotoxicity due to formation of bilirubin on oxidative conversion.[10] This has resulted in a surge of interest to develop a new generation of PDT drugs that are less toxic and photoactive at longer wavelengths near 800 nm considering greater tissue permeability of the longer wavelength radiations.[11−15] Besides, some nonmacrocyclic organic dyes are also found to be potentially suitable for PDT applications.[16,17] There are several bioactive organic molecules derived from antibiotics and peptides known to cleave DNA on photoirradiation at UV light.[18−20] Such molecules, however, lack any visible absorption band within the "phototherapeutic window" of 620−850 nm, thus making them unsuitable for PDT applications.

Transition-metal complexes with their varied coordination environments and versatile redox and spectral properties offer better scope of designing species that are suitable to photocleave DNA in visible light following different routes like type-1 and photoredox pathways in addition to the singlet oxygen (type-2) process.[21−23] Metal complexes are known to cleave DNA by oxidative and hydrolytic pathways. Metal ions with strong Lewis acidity cleave DNA by phosphodiester bond hydrolysis.[24−26] Oxidative cleavage of DNA occurs in the presence of additional oxidizing/reducing agents or by photochemical means.[27−30] Transition-metal complexes cleaving DNA on photoirradiation are of relevance to PDT when the photoactivation takes place in the PDT window of 620−850 nm.

Polypyridyl ruthenium(II) complexes are known to cleave DNA in visible light.[31−33] Dirhodium(II) complexes show oxidative cleavage of DNA in visible light via both oxygen-dependent and -independent pathways.[34−36] Such complexes are potential agents for PDT applications. We have shown that copper(II) complexes having DNA binders and photoactive ligands like dipyridoquinoxaline (dpq) and dipyridophenazine (dppz) cleave DNA in red light following different mechanistic pathways.[37−39]

The present work stems from our interest in designing new oxovanadium(IV) complexes that are capable of cleaving DNA in red light. Vanadium(IV) complexes with a $3d^1$ electronic configuration show low-energy visible bands like $3d^9$ copper(II) complexes. It is thus expected that V(IV) species could mimic the properties of its Cu(II) analogues in showing visible light-induced DNA cleavage activity in red light. Copper(II) complexes are known to show "chemical nuclease" activity in the presence of a reducing agent like ascorbic acid or 3-mercaptopropionic acid.[40] Significant dark toxicity of Cu(II) complexes in cellular applications is due to formation of Cu(I) species in the presence of reducing

(9) (a) Szacilowski, K.; Macyk, W.; Drzewiecka-Matuszek, A.; Brindell, M.; Stochel, G. *Chem. Rev.* **2005**, *105*, 2647. (b) Armitage, B. *Chem. Rev.* **1998**, *98*, 1171.

(10) Ochsner, M. *J. Photochem. Photobiol. B* **1996**, *32*, 3.

(11) (a) Peng, Q.; Warloe, T.; Berg, K.; Moan, J.; Kongshaug, M.; Giercsky, K.-E.; Nesland, J. M. *Cancer* **1997**, *79*, 2282. (b) Kennedy, J. C.; Pottier, R. H.; Pross, D. C. *J. Photochem. Photobiol. B* **1990**, *6*, 143.

(12) (a) Dilkes, M. G.; De Jode, M. L.; Rowntree-Taylor, A. *Lasers Med. Sci.* **1997**, *11*, 23. (b) Bonnett, R.; White, R. D.; Winfield, U.-J.; Berenbaum, M. C. *Biochem. J.* **1989**, *261*, 277.

(13) (a) Razum, N.; Snyder, A.; Dorion, D. *Proc. Soc. Photo-opt. Instrum. Eng.* **1996**, *2675*, 43. (b) Morgan, A. R.; Garbo, G. M.; Keck, R. W.; Selman, S. H. *Cancer Res.* **1988**, *48*, 194.

(14) (a) Nelson, J. S.; Roberts, W. G.; Berns, J. W. *Cancer Res.* **1987**, *47*, 4681. (b) Pandey, R. K.; Sumlin, A. B.; Constantine, S.; Aoudia, M.; Potter, W. R.; Bellnier, D. A.; Henderson, B. W.; Rodgers, M. A.; Smith, K. M.; Dougherty, T. J. *Photochem. Photobiol.* **1996**, *64*, 194. (c) Stranadko, E.; Skobelkin, O.; Litwin, G.; Astrakhankina, T. *Proc. Soc. Photo-opt. Instrum. Eng.* **1994**, *2325*, 240. (d) Richter, A. M.; Kelly, B.; Chow, J.; Liu, D. J.; Towers, G. M. N.; Dolphin, D.; Levy, J. G. *J. Natl. Cancer. Inst.* **1987**, *79*, 1327. (e) Levy, J. G.; Chan, A.; Strong, H. A. *Proc. Soc. Photo-opt. Instrum. Eng.* **1996**, *2625*, 86.

(15) Young, S. W.; Woodburn, K. W.; Wright, M.; Mody, T. D.; Fan, Q.; Sessler, J. L.; Dow, W. C.; Miller, R. A. *Photochem. Photobiol.* **1996**, *63*, 892.

(16) Atilgan, S.; Ekmekci, Z.; Dogan, A. L.; Guc, D.; Akkaya, E. U. *Chem. Commun.* **2006**, 4398.

(17) (a) McDonnell, S. O.; Hall, M. J.; Allen, L. T.; Byrne, A.; Gallagher, W. M.; O'Shea, D. F. *J. Am. Chem. Soc.* **2005**, *127*, 16360. (b) Killoran, J.; Allen, L.; Gallagher, J. F.; Gallagher, W. M.; O'Shea, D. F. *Chem. Commun.* **2002**, 1862.

(18) (a) Gillman, I. G.; Yezek, J. M.; Manderville, R. A. *Chem. Commun*. **1998**, 647. (b) Frier, C.; Mouscadet, J. F.; Decout, J. L.; Auclair, C.; Fontecave, M. *Chem. Commun*. **1998**, 2457. (c) Theodorakis, E. A.; Xiang, X.; Blom, P. *Chem. Commun*. **1997**, 1463. (d) Qian, X.; Huang, T.-B.; Wei, D.; Zhu, D.-H.; Fan, M.; Yao, W. *J. Chem. Soc., Perkin Trans.* **2000**, *2*, 715.

(19) (a) Toshima, K.; Takai, S.; Maeda, Y.; Takano, R.; Matsumura, S. *Angew. Chem., Int. Ed.* **2000**, *39*, 3656. (b) Schmittel, M.; Viola, G.; Dall'Acqua, F.; Morbach, G. *Chem. Commun.* **2003**, 646. (c) Breslin, D. T.; Coury, J. E.; Anderson, J. R.; McFail-Isom, L.; Kan, Y.; Williams, L. D.; Bottomley, L. A.; Schuster, G. B. *J. Am. Chem. Soc.* **1997**, *119*, 5043.

(20) (a) Mahon, K. P.; Ortiz-Meoz, R. F., Jr.; Meoz, O.; Prestwich, E. G.; Kelley, S. O. *Chem. Commun*. **2003**, 1956. (b) Kovalenko, S. V.; Alabugin, I. V. *Chem. Commun*. **2005**, 1444. (c) Bohne, C.; Faulhaber, K.; Giese, B.; Häfner, A.; Hofmann, A.; Ihmels, H.; Köhler, A.-K.; Perä, S.; Schneider, F.; Sheepwash, M. A. L. *J. Am. Chem. Soc.* **2005**, *127*, 76.

(21) Chifotides, H. T.; Dunbar, K. R. *Acc. Chem. Res.* **2005**, *38*, 146.

(22) (a) Erkkila, K. E.; Odom, D. T.; Barton, J. K. *Chem. Rev.* **1999**, *99*, 2777. (b) Delaney, S.; Pascaly, M.; Bhattacharya, P. K.; Han, K.; Barton, J. K. *Inorg. Chem.* **2002**, *41*, 1966.

(23) Arounaguiri, S.; Maiya, B. G. *Inorg. Chem.* **1996**, *35*, 4267.

(24) Wolkenberg, S. E.; Boger, D. L. *Chem. Rev.* **2002**, *102*, 2477.

(25) Sreedhara, A.; Cowan, J. A. *J. Biol. Inorg. Chem.* **2001**, *6*, 337.

(26) An, Y.; Liu, S.-D.; Deng, S.-Y.; Ji, L.-N.; Mao, Z.-W. *J. Inorg. Biochem.* **2006**, *100*, 1586.

(27) Burrows, C. J.; Muller, J. G. *Chem. Rev.* **1998**, *98*, 1109.

(28) Sigman, D. S.; Mazumder, A.; Perrin, D. M. *Chem. Rev.* **1993**, *93*, 2295.

(29) (a) Kraft, B. J.; Zaleski, J. M. *New J. Chem.* **2001**, *25*, 1281. (b) Umezawa, H. *Prog. Biochem. Pharmacol.* **1976**, *11*, 18.

(30) (a) Meunier, B. *Chem. Rev.* **1992**, *92*, 1411. (b) Reedijk, J. *J. Inorg. Biochem.* **2001**, *86*, 89.

(31) Miao, R.; Mongelli, M. T.; Zigler, D. F.; Winkel, B. S. J.; Brewer, K. J. *Inorg. Chem.* **2006**, *45*, 10413.

(32) Chouai, A.; Wicke, S. E.; Turro, C.; Bacsa, J.; Dunbar, K. R.; Wang, D.; Thummel, R. P. *Inorg. Chem.* **2005**, *44*, 5996.

(33) Hergueta-Bravo, A.; Jiménez-Hernández, M. E.; Montero, F.; Oliveros, E.; Orellana, G. *J. Phys. Chem. B* **2002**, *106*, 4010.

(34) Angeles-Boza, A. M.; Bradley, P. M.; Fu, P. K.-L.; Shatruk, M.; Hilfiger, M. G.; Dunbar, K. R.; Turro, C. *Inorg. Chem.* **2005**, *44*, 7262.

(35) Bradley, P. M.; Angeles-Boza, A. M.; Dunbar, K. R.; Turro, C. *Inorg. Chem.* **2004**, *53*, 2450.

(36) Angeles-Boza, A. M.; Bradley, P. M.; Fu, P. K.-L.; Wicke, S. E.; Bacsa, J.; Dunbar, K. R.; Turro, C. *Inorg. Chem.* **2004**, *43*, 8510.

(37) Dhar, S.; Senapati, D.; Reddy, P. A. N.; Das, P. K.; Chakravarty, A. R. *Chem. Commun.* **2003**, 2452.

(38) Dhar, S.; Nethaji, M.; Chakravarty, A. R. *Inorg. Chem.* **2006**, *45*, 11043.

(39) (a) Patra, A. K.; Nethaji, M.; Chakravarty, A. R. *Dalton Trans.* **2005**, 2798. (b) Patra, A. K.; Dhar, S.; Nethaji, M.; Chakravarty, A. R. *Dalton Trans.* **2005**, 896.

(40) (a) Sigman, D. S. *Acc. Chem. Res.* **1986**, *19*, 180. (b) Sigman, D. S.; Bruice, T. W.; Mazumder, A.; Sutton, C. L. *Acc. Chem. Res.* **1993**, *26*, 98.

thiols.[41] The Cu(I) species reacts with cellular oxygen to generate hydroxyl radicals and/or copper-bound oxo/hydroxo species that cleave DNA.[42] Copper complexes thus have limitations for PDT applications due to their dark toxicity. This drawback can be readily circumvented by choosing V(IV) as a substitute of Cu(II). Vanadium(IV) ion in VO^{2+} is unlikely to undergo facile redox transformation in a cellular medium. Again, VO^{2+} complexes show a d−d band near 700 nm. Additionally, vanadium is a biocompatible metal ion used earlier as insulin mimetics and antitumor agents.[43−46] Bleomycin vanadyl(IV) and $[VO(phen)(H_2O)_2]^{2+}$ show "chemical nuclease" activity in the presence of H_2O_2.[47,48] There are few reports on oxovanadium(V) and peroxovanadium(V) complexes cleaving DNA on photoactivation in UV-A light.[49−52] Photocleavage of DNA by vanadium complexes in red light is unprecedented in the literature. Herein, we present the synthesis, structure, DNA binding, and photoinduced DNA cleavage activity of new oxovanadium(IV) complexes [VO(salmet)(B)] (**1**−**3**) and [VO(saltrp)(B)] (**4**−**6**), where salmet and saltrp are *N*-salicylidene-L-methionate and *N*-salicylidene-L-tryptophanate, respectively, and B is a *N*,*N*-donor heterocyclic base (viz. 1,10-phenanthroline (phen, **1**, **4**), dipyrido[3,2-d:2′,3′-f]quinoxaline (dpq, **2**, **5**), and dipyrido[3,2-a:2′,3′-c]phenazine (dppz, **3**, **6**)) (Chart 1). The choice of planar phenanthroline bases is based on their good DNA binding ability and the photoactive nature of the quinoxaline and phenazine moieties. Bioessential photoactive α-amino acids are used for Schiff base preparation. Significant results include observation of a wide voltage window between two metal-based redox couples, poor "chemical nuclease" activity, and efficient photoinduced DNA cleavage activity of the dpq (**2**, **5**) and dppz (**3**, **6**) complexes in red light.

Chart 1. Ternary Structures of the VO^{2+} Complexes (**1**−**6**) and Phenanthroline Bases Used

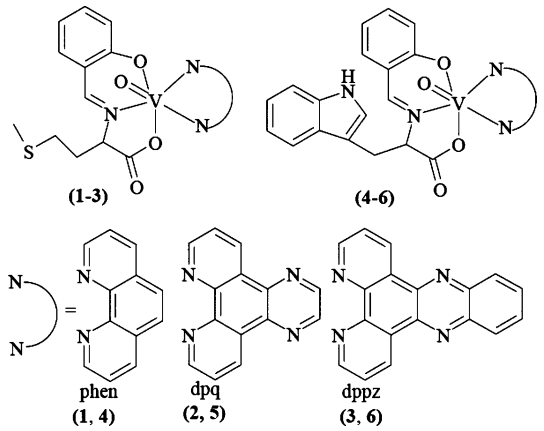

Experimental Section

Materials and Measurements. All reagents and chemicals were procured from commercial sources (SD Fine Chemicals, India; Aldrich) and used without further purifications. Solvents were purified by standard procedures.[53] Syntheses of the complexes were done under a nitrogen atmosphere using Schlenk techniques. Supercoiled (SC) pUC19 DNA (cesium chloride purified) was purchased from Bangalore Genie (India). Tris(hydroxylmethyl)-aminomethane-HCl (Tris-HCl) buffer solution was prepared using deionized and sonicated triple-distilled water. Calf thymus (CT) DNA, agarose (molecular biology grade), distamycin-A, catalase, superoxide dismutase (SOD), 2,2,6,6-tetramethyl-4-piperidone (TEMP), 1,4-diazabicyclo-[2.2.2]octan (DABCO), and ethidium bromide (EB) were from Sigma. The *N*,*N*-donor heterocyclic bases dipyrido-[3,2-d:2′,3′-f]-quinoxaline (dpq) and dipyrido[3,2-a:2′,3′-c]phenazine (dppz) were prepared by literature procedures using 1,10-phenanthroline-5,6-dione as a precursor reacted with ethylenediamine for dpq and 1,2-phenylenediamine for dppz.[54,55]

Elemental analysis was done using a Thermo Finnigan Flash EA 1112 CHNSO analyzer. Infrared and electronic spectra were recorded on Perkin-Elmer Lambda 35 and Perkin-Elmer Spectrum one 55 spectrophotometers, respectively. Molar conductivity measurements were performed using a Control Dynamics (India) conductivity meter. Room-temperature magnetic susceptibility data were obtained from a George Associates Inc. Lewis-coil force magnetometer using $Hg[Co(NCS)_4]$ as a standard. Experimental susceptibility data were corrected for diamagnetic contributions.[56] Cyclic voltammetric measurements were made at 25 °C on a EG&G PAR model 253 Versa Stat potentiostat/galvanostat with electrochemical analysis software 270 using a three-electrode setup comprised of glassy carbon working, platinum wire auxiliary, and saturated calomel reference (SCE) electrodes. Tetrabutylammonium perchlorate (TBAP, 0.1 M) was used as a supporting electrolyte in DMF. The electrochemical data were uncorrected for junction

(41) Reed, C. J.; Douglas, K. T. *Biochem. J.* **1991**, *275*, 601.
(42) Pogozelski, W. K.; Tullius, T. D. *Chem. Rev.* **1998**, *98*, 1089.
(43) (a) Crans, D. C.; Tracey, A. S. In *Vanadium Compounds: Chemistry, Biochemistry, and Therapeutic Applications*; Tracey, A. S., Crans, D. C., Eds.; American Chemical Society: Washington, DC, 1998; Vol. 711, pp 2−29. (b) Stankiewicz, P. J.; Tracey, A. S.; Crans, D. C. In *Vanadium and Its Role in Life, Metal Ions in Biological Systems*; Sigel, H., Sigel, A., Eds.; Marcel Dekker: New York 1995; Vol. 31, Chapter 9, pp 287−324.
(44) (a) Liasko, R.; Kabanos, T. A.; Karkabounas, S.; Malamas, M.; Tasiopoulos, J. A.; Stefanou, D.; Collery, P.; Evangelou, A. *Anticancer Res.* **1998**, *18*, 3609. (b) Evangelou, A. *Crit. Rev. Oncol. Hematol.* **2002**, *42*, 249.
(45) Rehder, D.; Pessoa, J. C.; Geraldes, C. F. G. C.; Castro, M. M. C. A.; Kabanos, T.; Kiss, T.; Meier, B.; Micera, G.; Pettersson, L.; Rangel, M.; Salifoglou, A.; Turel, I.; Wang, D. G. *J. Biol. Inorg. Chem.* **2002**, *7*, 675.
(46) Crans, D. C.; Yang, L. Q.; Alfano, J. A.; Chi, L. A. H.; Jin, W. Z.; Mahroof-Tahir, M.; Robbins, K.; Toloue, M. M.; Chan, L. K.; Plante, A. J.; Grayson, R. Z.; Willsky, G. R. *Coord. Chem. Rev.* **2003**, *237*, 13.
(47) Kuwahara, J.; Suzuki, T.; Sugiura, Y. *Biochem. Biophys. Res. Commun.* **1985**, *129*, 368.
(48) (a) Sakurai, H.; Tamura, H.; Okatani, K. *Biochem. Biophys. Res. Commun.* **1995**, *206*, 133. (b) Narla, R. K.; Dong, Y.; D'Cruz, O. J.; Navara, C.; Uckun, F. M. *Clin. Cancer Res.* **2000**, *6*, 1546. (c) Dong, Y.; Narla, R. K.; Sudbeck, E.; Uckun, F. M. *J. Inorg. Biochem.* **2000**, *78*, 321.
(49) Sam, M.; Hwang, J. H.; Chanfreau, G.; Abu-Omar, M. M. *Inorg. Chem.* **2004**, *43*, 8447.
(50) (a) Kwong, D. W. J.; Chan, O. Y.; Shek, L. K.; Wong, R. N. S. *J. Inorg. Biochem.* **2005**, *99*, 2062. (b) Kwong, D. W. J.; Chan, O. Y.; Wong, R. N. S.; Musser, S. M.; Vaca, L.; Chan, S. I. *Inorg. Chem.* **1997**, *36*, 1276.
(51) Hiort, C.; Goodisman, J.; Dabrowiak, J. C. *Biochemistry* **1996**, *35*, 12354.
(52) Chen, C.-T.; Lin, J.-S.; Kuo, J.-H.; Weng, S.-S.; Cuo, T.-S.; Lin, Y.-W.; Cheng, C.-C.; Huang, Y.-C.; Yu, J.-K.; Chou, P.-T. *Org. Lett.* **2004**, *6*, 4471.
(53) Perrin, D. D.; Armarego, W. L. F.; Perrin, D. R. *Purification of Laboratory Chemicals*; Pergamon Press: Oxford, 1980.
(54) Dickeson, J. E.; Summers, L. A. *Aus. J. Chem.* **1970**, *23*, 1023.
(55) Amouyal, E.; Homsi, A.; Chambron, J.-C.; Sauvage, J.-P. *J. Chem. Soc., Dalton Trans.* **1990**, 1841.
(56) Khan, O. *Molecular Magnetism*; VCH: Weinheim, 1993.

potentials. Electrospray ionization mass spectral measurements were done using Esquire 3000 plus ESI (Bruker Daltonics) and Q-TOF mass spectrometer.

Preparation of [VO(salmet)(B)] (1−3) and [VO(saltrp)(B)] (4−6) [B = phen (1, 3), dpq (2, 4), dppz (3, 6)]. Complexes **1**−**6** were prepared by a general synthetic procedure in which a mixture of the corresponding α-amino acid [L-met (0.15 g, 1.0 mmol); L-trp (0.20 g, 1.0 mmol)] and NaOH (0.03 g, 0.75 mmol) in 10 mL water were added to a methanolic solution of salicylaldehyde (0.10 mL, 1.0 mmol). The resulting solution was refluxed for 1 h, followed by addition of an aqueous solution of vanadyl sulfate (0.16 g, 1.0 mmol). A light-bluish precipitate was obtained after refluxing the mixture for 1 h. To this mixture was added the corresponding heterocyclic base [0.20 g, phen; 0.23 g, dpq; 0.29 g, dppz (1.0 mmol)] taken in 10 mL of methanol. The solution on further refluxing for 1 h gave a red precipitate. The solid was isolated, washed with MeOH, and finally dried in vacuum over P_4O_{10}. Yield: ∼75%. Anal. Calcd for $C_{24}H_{21}N_3O_4SV$ (**1**): C, 57.83; H, 4.25; N, 8.43; S, 6.43. Found: C, 57.72; H, 4.21; N, 8.41; S, 6.42. ESI-MS in MeCN: *m*/*z* 499 $[M + H]^+$. $\Lambda_M = 10$ S m^2 M^{-1} in DMF at 25 °C. IR (KBr phase, cm^{-1}): 3446br, 2918w, 1650vs, 1619vs (C═N), 1536m, 1466w, 1445m, 1425m, 1341m, 1199w, 1148w, 960s (V═O), 849m, 775w, 726w (br, broad; vs, very strong; s, strong; m, medium; w, weak). UV−vis in DMF [λ_{max}/nm (ϵ/M^{-1} cm^{-1})]: 844sh (20), 708 (35), 470 (800), 380 (4820), 267 (44 160) (sh, shoulder). $\mu_{eff} = 1.65$ μ_B at 298 K. Anal. Calcd for $C_{26}H_{21}N_5O_4SV$ (**2**): C, 56.73; H, 3.85; N, 12.72; S, 5.83. Found: C, 56.68; H, 3.83; N, 12.69; S, 5.77. ESI-MS in MeCN: *m*/*z* 551 $[M + H]^+$. $\Lambda_M = 7$ S m^2 M^{-1} in DMF at 25 °C. IR (KBr phase, cm^{-1}): 3446w, 2921w, 1651vs, 1621vs (C═N), 1532w, 1466w, 1441m, 1403m, 1343w, 1198w, 1083w, 962s (V═O), 809w, 765w. UV−vis in DMF [λ_{max}/nm (ϵ/M^{-1} cm^{-1})]: 848sh (30), 701 (40), 469 (605), 376 (5400), 341 (7630), 325 (8490), 270 (38 860). $\mu_{eff} = 1.70$ μ_B at 298 K. Anal. Calcd for $C_{30}H_{23}N_5O_4SV$ (**3**): C, 60.00; H, 3.86; N, 11.66; S, 5.34. Found: C, 59.95; H, 3.85; N, 11.58; S, 5.56. ESI-MS in MeCN: *m*/*z* 601 $[M + H]^+$. $\Lambda_M = 4$ S m^2 M^{-1} in DMF at 25 °C. IR (KBr phase, cm^{-1}): 3466br, 2920w, 1641s, 1618vs (C═N), 1537m, 1495w, 1445m, 1339m, 1197w, 1149w, 1076w, 960s (V═O), 808w, 763w. UV−vis in DMF [λ_{max}/nm (ϵ/M^{-1} cm^{-1})]: 840sh (20), 694 (40), 460 (915), 380 (18 220), 362 (17 080), 270 (16 100). $\mu_{eff} = 1.68$ μ_B at 298 K. Anal. Calcd for $C_{30}H_{22}N_4O_4V$ (**4**): C, 65.10; H, 4.01; N, 10.12. Found: C, 64.86; H, 3.96; N, 10.22. ESI-MS in MeCN: *m*/*z* 554 $[M + H]^+$. $\Lambda_M =$ 3 S m^2 M^{-1} in DMF at 25 °C. IR (KBr phase, cm^{-1}): 3217w, 3056w, 2909w, 1623vs (C═N), 1539w, 1447w, 1343m, 1152w, 959s (V═O), 845w, 751w. UV−vis in DMF [λ_{max}/nm (ϵ/M^{-1} cm^{-1})]: 840sh (16), 691 (30), 473 (670), 375 (4960), 269 (41 370). $\mu_{eff} = 1.62$ μ_B at 298 K. Anal. Calcd for $C_{32}H_{22}N_6O_4V$ (**5**): C, 63.48; H, 3.66; N, 13.88. Found: C, 63.66; H, 3.49; N, 13.85. ESI-MS in MeCN: *m*/*z* 606 $[M + H]^+$. $\Lambda_M = 4$ S m^2 M^{-1} in DMF at 25 °C. IR (KBr phase, cm^{-1}): 3440br, 3067w, 2919w, 1627vs (C═N), 1540m, 1442m, 1369w, 1338w, 1300w, 1207w, 1081w, 999m, 961s (V═O), 817w, 755m. UV−vis in DMF [λ_{max}/nm (ϵ/M^{-1} cm^{-1})]: 841sh (20), 675 (40), 470 (760), 372 (5270), 341 (8410), 326 (9350), 267 (40 260). $\mu_{eff} = 1.66$ μ_B at 298 K. Anal. Calcd for $C_{36}H_{24}N_6O_4V$ (**6**): C, 65.96; H, 3.69; N, 12.82. Found: C, 65.75; H, 3.61; N, 12.91. ESI-MS in MeCN: *m*/*z* 656 $[M + H]^+$. $\Lambda_M = 2$ S m^2 M^{-1} in DMF at 25 °C. IR (KBr phase, cm^{-1}): 3431br, 3078w, 2927w, 1623vs (C═N), 1540w, 1447w, 1353m, 1202w, 1150w, 1077w, 964s (V═O), 818w, 739m. UV−vis in DMF [λ_{max}/nm (ϵ/M^{-1} cm^{-1})]: 838sh (20), 686 (40), 458 (910), 380 (21 650), 362 (20 695), 269 (90 410). $\mu_{eff} = 1.63$ μ_B at 298 K.

Solubility and Stability. The complexes were highly soluble in DMF and DMSO, less soluble in MeOH, MeCN, and H_2O, and insoluble in hydrocarbon solvents. They were stable in the solid and solution phases.

X-ray Crystallographic Procedures. Crystal structures of **1**, **2**, and **4** were obtained by single-crystal X-ray diffraction technique. Crystals were obtained from MeOH−CH_2Cl_2 solutions (1:1 v/v) of the complexes on slow evaporation of the solvent. Crystal mounting was done on glass fiber with epoxy cement. All geometric and intensity data were collected at room temperature using an automated Bruker SMART APEX CCD diffractometer equipped with a fine focus 1.75 kW sealed tube Mo Kα X-ray source (λ = 0.71073 Å) with increasing ω (width of 0.3° per frame) at a scan speed of 8, 15, and 13 s per frame for complexes **1**, **2**, and **4**, respectively. Intensity data, collected using the $\omega-2\theta$ scan mode, were corrected for Lorentz−polarization effects and absorption.[57] Structures were solved by the combination of Patterson and Fourier techniques and refined by full-matrix least-squares method using the SHELX system of programs.[58] All hydrogen atoms belonging to the complex were in their calculated positions and refined using a riding model. All non-hydrogen atoms were refined anisotropically. Perspective views of the molecules were obtained by ORTEP.[59]

DNA Binding Methods. The experiments were carried out in Tris-HCl buffer (50 mM Tris-HCl, pH 7.2) using the complex solution in DMF (10%). The calf thymus (CT) DNA (ca. 350 μM NP) in the buffer medium gave a ratio of UV absorbance at 260 and 280 nm of ca. 1.9:1, suggesting the DNA was apparently free from protein. The concentration of DNA was estimated from its absorption intensity at 260 nm with a known molar absorption coefficient value of 6600 M^{-1} cm^{-1}.[60] Absorption titration experiments were performed by varying the concentration of the CT DNA while keeping the complex concentration constant. Due correction was made for the absorbance of DNA itself. The spectra were recorded after equilibration for 5 min. The intrinsic equilibrium binding constant (K_b) and binding site size (*s*) of the complexes to CT DNA were obtained by the McGhee−von Hippel (MvH) method using the expression of Bard and co-workers by monitoring the change of the absorption intensity of the spectral bands with increasing concentration of CT DNA by regression analysis using eq 1

$$(\epsilon_a - \epsilon_f)/(\epsilon_b - \epsilon_f) = (b - (b^2 - 2K_b{}^2C_t[\mathrm{DNA}]_t/s)^{1/2})/2K_bC_t \qquad (1)$$

$$b = 1 + K_bC_t + K_b[\mathrm{DNA}]_t/2s$$

where ϵ_a is the extinction coefficient observed for the charge-transfer absorption band at a given DNA concentration, ϵ_f is the extinction coefficient of the complex free in solution, ϵ_b is the extinction coefficient of the complex when fully bound to DNA, K_b is the equilibrium binding constant, C_t is the total metal complex concentration, $[\mathrm{DNA}]_t$ is the DNA concentration in nucleotides, and *s* is the binding site size in base pairs.[61,62] The nonlinear least-squares analysis was done using Origin Lab, version 6.1.

(57) Walker, N.; Stuart, D. *Acta Crystallogr.* **1993**, *A39*, 158.
(58) Sheldrick, G. M. *SHELX-97*, *Programs for Crystal Structure Solution and Refinement*; University of Göttingen: Göttingen, Germany, 1997.
(59) Johnson, C. K. *ORTEP*, *Report ORNL-5138*; Oak Ridge National Laboratory: Oak Ridge, TN, 1976.
(60) Reichman, M. E.; Rice, S. A.; Thomas, C. A.; Doty, P. *J. Am. Chem. Soc.* **1954**, *76*, 3047.
(61) McGhee, J. D.; von Hippel, P. H. *J. Mol. Biol.* **1974**, *86*, 469.
(62) Carter, M. T.; Rodriguez, M.; Bard, A. J. *J. Am. Chem. Soc.* **1989**, *111*, 8901.

Table 1. Physicochemical Data for Complexes **1**−**6**

complex	IR,[a] cm^{-1} ν(V═O)	IR,[a] cm^{-1} ν(C═N)	λ, nm (ϵ, M^{-1} cm^{-1})[b]	μ_{eff}[c]	ΔT_m[d]/°C	K_b/M^{-1} (s)[e]
[VO(salmet)(phen)] (**1**)	960	1619	844 (20),[f] 708 (35)	1.65	1.5	0.5(±0.1) × 10^5 [0.1]
[VO(salmet)(dpq)] (**2**)	962	1621	848 (30),[f] 701 (40)	1.70	2.5	2.7(±0.6) × 10^5 [0.1]
[VO(salmet)(dppz)] (**3**)	960	1618	840 (20),[f] 694 (40)	1.68	4.08	7.2(±0.6) × 10^5 [0.3]
[VO(saltrp)(phen)] (**4**)	959	1623	840 (16),[f] 691 (30)	1.62	1.5	0.6(±0.1) × 10^5 [0.1]
[VO(saltrp)(dpq)] (**5**)	961	1627	841 (20),[f] 675 (40)	1.66	2.48	1.1(±0.2) × 10^5 [0.1]
[VO(saltrp)(dppz)] (**6**)	964	1623	838 (20),[f] 686 (40)	1.63	3.28	3.4(±0.7) × 10^5 [0.1]

[a] In KBr phase. [b] Visible electronic bands in DMF. [c] μ_{eff} in μ_B for solid powdered samples at 298 K. [d] Change in the DNA melting temperature. [e] K_b, DNA binding constant (s, binding site size). [f] Shoulder.

DNA melting experiments were carried out by monitoring the absorption intensity of CT DNA (180 μM) at 260 nm at various temperatures both in the absence and in the presence of the oxovanadium(IV) complexes (30 μM). Measurements were carried out using a Perkin-Elmer Lambda 35 spectrophotometer equipped with a Peltier temperature-controlling programmer (PTP 6) (±0.1 °C) on increasing the temperature of the solution by 0.5 °C/min. Viscometric titrations were performed with a Schott Gerate AVS 310 Automated Viscometer. The viscometer was thermostated at 37 °C in a constant temperature bath. The concentration of CT DNA was 135 μM in NP, the flow times were measured with an automated timer, each sample was measured three times, and an average flow time was calculated. Data were presented as $(\eta/\eta_0)^{1/3}$ vs [complex]/[DNA], where η is the viscosity of DNA in the presence of complex and η_0 is that of DNA alone. Viscosity values were calculated from the observed flowing time of DNA-containing solutions (t) corrected for that of the buffer alone (t_0), $\eta = (t - t_0)$.

DNA Cleavage Experiments. The cleavage of supercoiled pUC19 DNA (33.3 μM, 0.2 μg, 2686 base pair) was studied by agarose gel electrophoresis using metal complexes in 50 mM tris(hydroxylmethyl)methane-HCl (Tris-HCl) buffer (pH 7.2) containing 50 mM NaCl. For photoinduced DNA cleavage studies, the reactions were carried out under illuminated conditions using UV-A source at 365 nm (12 W, model LF-206.LS) or near IR light of ∼750 nm using a Spectra Physics Water-Cooled Mixed-Gas Ion Laser Stabilite2018-RM (continuous-wave (CW) beam diameter at 1/e^2 1.8 mm ± 10% and beam divergence with full angle 0.7 mrad ± 10%) with an attachment model 2018-RM-IR with all-lines IR optics (752.5−799.3 nm). The laser beam power at the sample position (5 cm from the aperture with a solution path length of 5 mm) was 150 mW, measured using a Spectra Physics CW Laser Power Meter (model 407A). After light exposure, each sample was incubated for 1.0 h at 37 °C and analyzed for the photocleaved products using gel electrophoresis. The mechanistic studies were carried out using different additives (NaN_3, 0.5 mM; DMSO, 4 μL; catalase, 4 units; SOD, 4 units; TEMP, 0.5 mM; DABCO, 0.5 mM) prior to addition of the complex. For the D_2O experiment, this solvent was used for dilution of the sample to 18 μL. The samples after incubation in a dark chamber were added to the loading buffer containing 25% bromophenol blue, 0.25% xylene cyanol, and 30% glycerol (3 μL), and the solution was finally loaded on 0.8% agarose gel containing 1.0 μg/mL ethidium bromide. Electrophoresis was carried out in a dark chamber for 2.0 h at 60 V in TAE (Tris-acetate EDTA) buffer. Bands were visualized by UV light and photographed. The extent of DNA cleavage was measured from the intensities of the bands using a UVITEC Gel Documentation System. Due corrections were made for the low level of nicked circular (NC) form present in the original supercoiled (SC) DNA sample and for the low affinity of EB binding to SC compared to NC and linear forms of DNA.[63] The concentrations of the complexes and additives corresponded to that in the 18 μL final volume of the sample using Tris buffer. The observed error in measuring the band intensities was ∼5%.

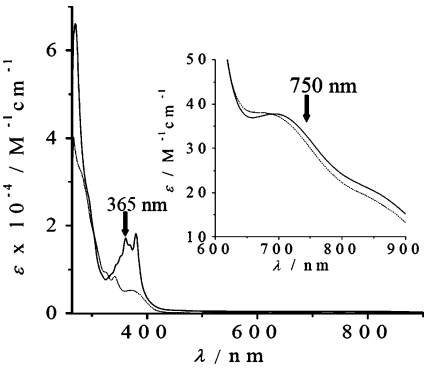

Figure 1. Electronic absorption spectra of [VO(salmet)(dpq)] (**3**) (—) and [VO(saltrp)(dppz)] (**5**) (- - -) in DMF. Wavelengths (365 and 750 nm) used for DNA photocleavage experiments are shown by the arrows.

Results and Discussion

Synthesis and General Aspects. Complexes of formulations [VO(salmet)(B)] (B = phen, **1**; dpq, **2**; dppz, **3**) and [VO(saltrp)(B)] (B = phen, **4**; dpq, **5**; dppz, **6**) are prepared in high yield from a general synthetic procedure in which vanadyl sulfate is reacted with dianionic α-amino acid Schiff bases and phenanthroline bases in aqueous methanol (Chart 1). Selected physicochemical data for the complexes are given in Table 1. The nonelectrolytic complexes are soluble in aqueous DMF. They show characteristic vanadyl (V═O) and imine (C═N) infrared bands at ∼960 and ∼1620 cm^{-1}, respectively. They are one-electron paramagnetic, giving a magnetic moment value in the range from 1.6 to 1.7 μ_B at 25 °C in accordance with the 3d^1 electronic configuration of the $V^{IV}O^{2+}$ moiety. The electronic absorption spectra of the oxovanadium(IV) complexes **1**−**6** in DMF show two low-energy low-intensity metal-centered transitions near 840 and 700 nm (Figure 1). The band at >800 nm appears as a shoulder. The ∼700 nm band is used for the photoinduced DNA cleavage studies. An additional metal-centered band is observed near 470 nm. The molar extinction coefficient (ϵ) values for the low-energy bands that lie in the range of 15−40 M^{-1} cm^{-1} are significantly lower than analogous copper(II) complexes (ϵ values of ∼150 M^{-1} cm^{-1}), showing red-light-induced DNA cleavage activity.[37−39] It is thus of

(63) Bernadou, J.; Pratviel, G.; Bennis, F.; Girardet, M.; Meunier, B. *Biochemistry* **1989**, *28*, 7268.

Table 2. Electrochemical Data[a] for Complexes **1**−**6**

	anodic scan				cathodic scan		
complex	E_{pa}^1, V	E_{pc}^1, V	i_{pc}/i_{pa}	E_{pa}^2, V[b]	$E_{1/2}^1$,V (ΔE_p, mV)[c]	E_{pc}^2, V[d]	$E_{1/2}^2$,V (ΔE_p, mV)[e]
[VO(salmet)(phen)] (**1**)	0.86	0.44	0.3	1.25	−1.25 (80)	−1.37	
[VO(salmet)(dpq)] (**2**)	0.84	0.44	0.4	1.18	−1.14 (80)		−1.54 (70)
[VO(salmet)(dppz)] (**3**)	0.85	0.43	0.3	1.14	−0.96 (83)		−1.23 (65)
[VO(saltrp)(phen)] (**4**)	0.84	0.42	0.4	1.14	−1.29 (84)	−1.39	
[VO(saltrp)(dpq)] (**5**)	0.85	0.43	0.3	1.09	−1.19 (84)		−1.57 (65)
[VO(saltrp)(dppz)] (**6**)	0.85	0.42	0.3	1.13	−0.95 (77)		−1.11 (65)

[a] Scan rate of 50 mV s^{-1} in DMF−0.1 M TBAP. Potentials are vs saturated calomel electrode (SCE). $E_{1/2} = 0.5(E_{pa} + E_{pc})$. $\Delta E_p = (E_{pa} - E_{pc})$, where E_{pa} and E_{pc} are anodic and cathodic peak potentials, respectively. Currents i_{pc} and i_{pa} are for the cathodic and anodic peaks, respectively. [b] Anodic peak without any cathodic counterpart. [c] Quasi-reversible process with a i_{pc}/i_{pa} ratio of unity. [d] Cathodic peak without any anodic counterpart. [e] Quasi-reversible process with i_{pc}/i_{pa} ratio in the range of 0.8−0.9.

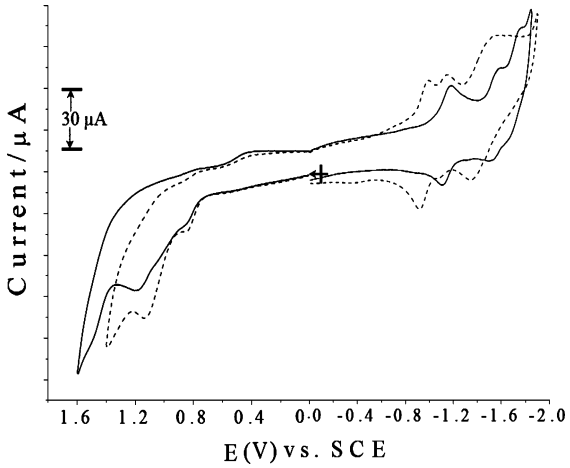

Figure 2. Cyclic voltammograms of [VO(salmet)(dpq)] (**2**) (—) and [VO(saltrp)(dppz)] (**6**) (- - -) in DMF−0.1 M TBAP at a scan speed of 50 mV s^{-1}.

interest to explore the utility of these vanadyl(IV) complexes in DNA cleavage studies at red light of >700 nm since compounds showing photocleavage of DNA at near IR wavelength are rare in the literature.[1] Lutetium(III) texaphyrin complex (LUTRIN) has a band at 732 nm, and this complex is under clinical trials for PDT applications.[15] Complexes **1**−**6** exhibit an intense band at ∼380 nm due to a ligand-to-metal charge-transfer (LMCT, $PhO^- \rightarrow V$) transition, and the remaining bands appearing in the UV region are assignable to the intraligand transitions.[64] All complexes display a band at ca. 270 nm assignable to the $\pi \rightarrow \pi^*$ transition. The complexes of the dpq and dppz ligands are known to exhibit an additional band near 350 nm due to n $\rightarrow \pi^*$ transition involving the quinoxaline and phenazine moieties.[65]

Electrochemistry. Complexes **1**−**6** are redox active, showing cyclic voltammetric responses involving the metal center and ligands in DMF−0.1 M TBAP (Table 2, Figure 2). Two anodic responses (E_{pa}) are observed near 0.8 and 1.2 V with a weak cathodic counterpart (E_{pc}) at ca. 0.4 V. The first anodic response is assigned to the V(V)/V(IV) redox couple showing a i_{pc}/i_{pa} peak current ratio of ∼0.4 (i_{pc} and i_{pa} are cathodic and anodic peak currents, respectively). The irreversible nature of the electron-transfer process involving the $V^VO^{3+}/V^{IV}O^{2+}$ moieties could be due to the unstable nature of the oxidized species in the presence of π-acceptor phenanthroline bases. The anodic peak at ∼1.2 V is broad in nature and could be due to ligand-based oxidation. The complexes display a quasi-reversible voltammetric response in the potential range from −0.9 to −1.3 V with a peak-to-peak (ΔE_p) separation of 70−84 mV at a 50 mV s^{-1} scan rate. This redox process is assignable to the V(IV)/V(III) couple. The observed voltage window of ∼2.0 V between the V(V)/V(IV) and V(IV)/V(III) couples is of significance. These complexes are expected to show poor "chemical nuclease" activity due to this voltage window. In contrast, analogous copper(II) complexes having a readily accessible metal-based Cu(II)/Cu(I) redox couple show significant "chemical nuclease" activity in the presence of reducing thiols.[41] Complexes **1**−**6** show ligand-based reductions. While the phen complexes display one irreversible reduction near −1.4 V, the dpq and dppz complexes display two redox processes. The first ligand-based redox process, observed for the dpq and dppz complexes near −1.5 and −1.1 V, respectively, with an ΔE_p value of ∼60 mV at 50 mV s^{-1}, is reversible in nature. An additional reductive response is observed near −1.7 and −1.4 V for the dpq and dppz ligands, respectively.

Crystal Structures. The phen and dpq complexes of the salmet ligand (**1**·2H_2O and **2**) and the phen complex of the saltrp ligand (**4**·0.5MeOH) are structurally characterized by single-crystal X-ray diffraction. Selected crystallographic data are summarized in Table 3. ORTEP views of the complexes are shown in Figures 3 and 4. Selected bond distances and angles are given in Table 4. The structure of the complexes consists of a discrete monomeric vanadium(IV) species with a VO^{2+} moiety bonded to a dianionic tridentate Schiff base ligand and a *N*,*N*-donor phenanthroline base (phen, dpq). The Schiff bases are bound through the phenolate oxygen, imine nitrogen, and carboxylate oxygen atoms, leaving the thiomethyl of salmet and indole ring of saltrp as the pendant groups. The lattice water molecules in **1**·2H_2O are involved in intermolecular bifurcated H-bonding interactions with the carboxylate oxygen atom of the Schiff base and the vanadyl oxygen atom giving distances in the range of 2.80−2.87 Å. The lattice methanol molecule in **4** shows intermolecular H-bonding interactions (distance = 2.74 Å) with the carboxylate oxygen atom of the Schiff base. In addition, the −NH of the indole ring of the saltrp ligand is involved in

(64) Dutta, S. K.; Kumar, S. B.; Bhattacharyya, S.; Tiekink, E. R. T.; Chaudhury, M. *Inorg. Chem.* **1997**, *36*, 4954.
(65) Toshima, K.; Takano, R.; Ozawa, T.; Matsumura, S. *Chem. Commun.* **2002**, 212.

Table 3. Selected Crystallographic Data for **1**·$2H_2O$, **2**, and **4**·0.5 CH_3OH

	1·$2H_2O$	**2**	**4**·0.5 CH_3OH
formula	$C_{24}H_{25}N_3O_6SV$	$C_{26}H_{21}N_5O_4SV$	$C_{30.5}H_{24}N_4O_{4.5}V$
cryst size (mm^3)	0.15 × 0.12 × 0.10	0.10 × 0.08 × 0.06	0.20 × 0.12 × 0.05
fw, g M^{-1}	534.47	550.48	569.48
cryst syst	orthorhombic	orthorhombic	orthorhombic
space group (no.)	$P2_12_12_1$ (19)	$P2_12_12_1$ (19)	$P2_12_12_1$ (19)
a, Å	10.000(3)	9.429(8)	10.420(7)
b, Å	15.541(4)	14.957(12)	16.214(10)
c, Å	15.830(4)	17.702(16)	31.66(2)
$\alpha = \beta = \gamma$, deg	90.0	90.0	90.0
V, $Å^3$	2460.2(11)	2497(4)	5350(6)
Z	4	4	8
T, K	293(2)	293(2)	293(2)
D (calcd) (g cm^{-3})	1.443	1.465	1.414
λ, Å (Mo Kα)	0.71073	0.71073	0.71073
μ (mm^{-1})	0.533	0.524	0.417
data/restraints/params	4575/0/316	4600/0/335	9873/0/721
goodness-of-fit on F^2	1.028	1.050	1.036
R (F_o)[a] [$I > 2\sigma(I)$]	0.0780	0.0759	0.0959
wR (F_o)[b] [$I > 2\sigma(I)$]	0.1176	0.1042	0.1444
R [all data] (wR [all data])	0.1503 (0.1375)	0.1235 (0.1175)	0.2031 (0.1819)
largest diff. peak and hole (e $Å^{-3}$)	0.452, −0.241	0.551, −0.228	0.456, −0.284
$w = 1/[\sigma^2(F_o^2)+(AP)^2+(BP)]$	$A = 0.0432$; $B = 0.0000$	$A = 0.0353$; $B = 0.0000$	$A = 0.0540$; $B = 0.0000$

[a] $R = \Sigma||F_o| - |F_c||/\Sigma|F_o|$. [b] $wR = \{\Sigma[w(F_o^2 - F_c^2)^2]/\Sigma[w(F_o)^2]\}^{1/2}$; $w = [\sigma^2(F_o)^2 + (AP)^2 + BP]^{-1}$, $P = (F_o^2 + 2F_c^2)/3$.

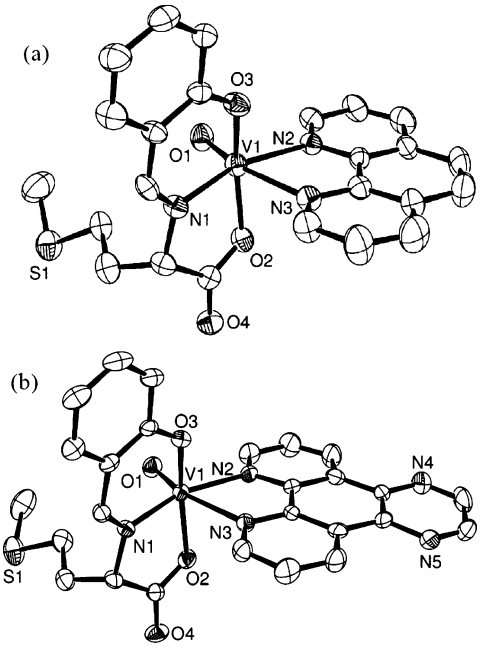

Figure 3. ORTEP views of [VO(salmet)(phen)] (**1**) (a) and [VO(salmet)-(dpq)] (**2**) (b) showing atom labeling for the metal and heteroatoms and 30% probability thermal ellipsoids.

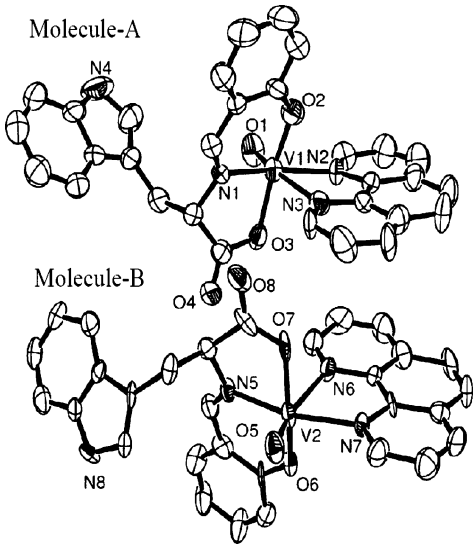

Figure 4. ORTEP views of two independent molecules of [VO(saltrp)-(phen)] (**4**) showing atom labeling for the metal and heteroatoms and 50% probability thermal ellipsoids.

an intermolecular H-bonding interaction with the carboxylate oxygen atom, giving a distance of 2.85 Å. The complexes have a $V^{IV}O_3N_3$ coordination geometry with the vanadyl group showing a V═O distance of ∼1.6 Å. The Schiff bases exhibit a meridional binding mode, leaving the phenanthroline base to bind at the axial−equatorial positions. The V−N bond trans to the V═O group is significantly long (2.33−2.36 Å) compared to the other V−N distances (∼2.15 and ∼2.05 Å). The V−O distances involving the Schiff bases are ∼2.0 Å. The molecular structure does not show any significant steric encumbrance of the phenanthroline base by the Schiff base ligands.

DNA Binding. Absorption titration method is used to monitor the interaction of complexes **1**−**6** with CT DNA (Table 1, Figure 5). A complex generally shows hypochromism and a red shift (bathochromism) of the absorption band when it binds to DNA through intercalation, resulting in a strong stacking interaction between the aromatic chromophore of the ligand and the base pairs of the DNA. The extent of hypochromism gives a measure of the strength of an intercalative binding. The observed trend in hypochromism among the present complexes follows the order dppz complexes **3**, **6** > dpq complexes **2**, **5** > phen complexes **1**, **4**. The intrinsic equilibrium DNA binding constant (K_b) values of the complexes along with the binding site size (*s*) are given in Table 1. The K_b values of $\sim 10^5$ M^{-1} follow the same order as observed in the trend of hypochromism. The binding site size (*s*) values obtained from the MvH fits are in the range of 0.1−0.3 with the dppz complexes showing a higher value of *s* in comparison to their dpq and phen analogues. This could be due to the

Table 4. Selected Bond Distances (Å) and Angles (deg) for [VO(salmet)(phen)] (**1**·2H_2O), [VO(salmet)(dpq)] (**2**), and [VO(saltrp)(phen)] (**4**·0.5 CH_3OH) with esd's in the Parentheses

	1·2H_2O	**2**	**4**·0.5 CH_3OH[a]
V(1)−O(1)	1.595(4)	1.591(4)	1.585(5)
V(1)−O(2)	1.996(4)	1.992(4)	1.958(6)
V(1)−O(3)	1.948(4)	1.951(4)	2.004(6)
V(1)−N(1)	2.046(5)	2.055(4)	2.059(7)
V(1)−N(2)	2.149(5)	2.168(5)	2.156(7)
V(1)−N(3)	2.333(5)	2.362(5)	2.335(7)
O(1)−V(1)−O(2)	100.8(2)	101.65(18)	102.4(3)
O(1)−V(1)−O(3)	100.7(2)	101.22(18)	101.2(3)
O(1)−V(1)−N(1)	103.4(2)	104.52(18)	103.7(3)
O(1)−V(1)−N(2)	93.3(2)	92.07(18)	93.6(3)
O(1)−V(1)−N(3)	165.8(2)	164.05(17)	166.3(3)
N(2)−V(1)−N(3)	72.6(2)	72.03(18)	73.0(3)

[a] The data correspond to the parameters observed in Molecule A in the asymmetric unit. The bonding parameters in Molecule B are similar to those in Molecule A [V(2)−O(5), 1.571(5) Å].

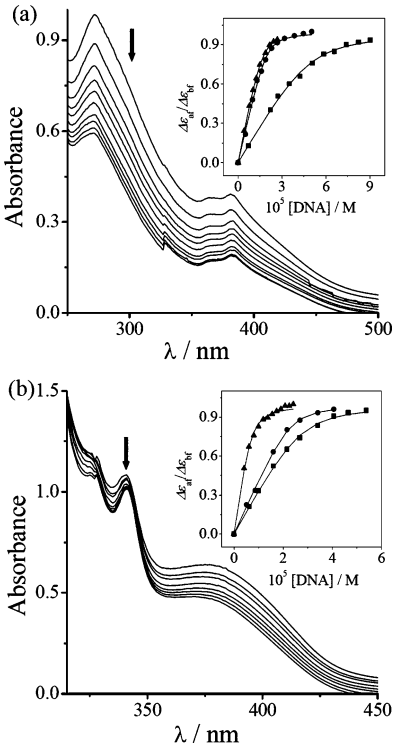

Figure 5. Absorption spectral traces of complexes **3** (a) and **5** (b) in 5 mM Tris-HCl buffer (pH 7.2) on increasing the quantity of CT DNA with the inset showing the least-squares fit of $\Delta\epsilon_{af}/\Delta\epsilon_{bf}$ vs [DNA] for **1** (■), **2** (●), and **3** (▲) (a) and **4** (■), **5** (●), and **6** (▲) (b) using the MvH equation (see text).

difference in their groove binding preferences. While the dppz ligand prefers DNA major groove binding, the dpq and phen ligands bind at the minor groove of DNA.[22] The Schiff base salmet shows a higher binding propensity than its saltrp analogue, possibly due to less steric bulk of the pendant thiomethyl group of methionine in comparison to the pendant indole ring of tryptophan. The small value of binding site size (*s*) suggests greater surface aggregation/groove binding of the complexes than intercalative binding mode to DNA.

Binding of complexes **1**−**6** to CT DNA was also studied from thermal denaturation and viscosity measurements (Table 1, Figure 6). A small change in the DNA melting temperature (ΔT_m) is observed on addition of the complexes to CT DNA. The low ΔT_m values for **1**−**6** suggest groove and/or

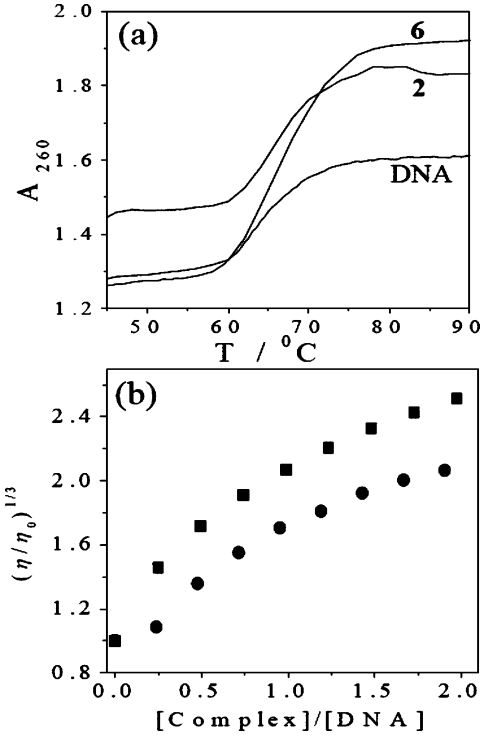

Figure 6. (a) Thermal denaturation plots of 180 μM CT DNA alone and in the presence of complexes **2** and **6**. (b) Effect of increasing amount of **3** (●) and **5** (■) on the relative viscosities of CT-DNA at 37.0 (±0.1) °C in 5 mM Tris-HCl buffer (pH, 7.2) ([DNA] = 135 μM, R = [complex]/[DNA]).

electrostatic binding of the complexes to CT DNA stabilizing the DNA double-helix structure in preference to an intercalative mode of binding to DNA that normally gives large positive ΔT_m values.[26,66] The surface aggregation may be promoted in the presence of the vanadyl (VO^{2+}) moiety of the complexes. Viscosity measurements are carried out to examine the effect on the specific relative viscosity of DNA upon addition of complexes. Since the relative specific viscosity (η/η_0) of DNA gives a measure of the increase in contour length associated with the separation of DNA base pairs caused by intercalation, a classical DNA intercalator like ethidium bromide shows a significant increase in the viscosity of DNA solutions (η and η_0 are the specific viscosities of DNA in the presence and absence of the complexes, respectively). In contrast, a partial and/or non-intercalation of the ligand could result in a less pronounced effect on the viscosity.[67] The plot of the relative specific viscosity $(\eta/\eta_0)^{1/3}$ versus [complex]/[DNA] ratio shows only a minor change in the viscosity. The results indicate the primarily DNA groove and/or surface binding nature of the complexes, giving an order of the (η/η_0) values as **3** > **2** > **1** and **6** > **5** > **4**.

Chemical Nuclease Activity. The oxidative cleavage of SC pUC19 DNA (33.3 μM) by complexes **1**−**6** (66.6 μM) in Tris-HCl/NaCl medium is studied under dark conditions using 3-mercaptopropionic acid (MPA, 0.5 mM) and glutathione (0.5 mM) as reducing agents and hydrogen peroxide (0.5 mM) as an oxidizing agent. The complexes are found

(66) Gunther, L. E.; Yong, A. S. *J. Am. Chem. Soc.* **1968**, *90*, 7323.
(67) Veal, J. M.; Rill, R. L. *Biochemistry* **1991**, *30*, 1132.

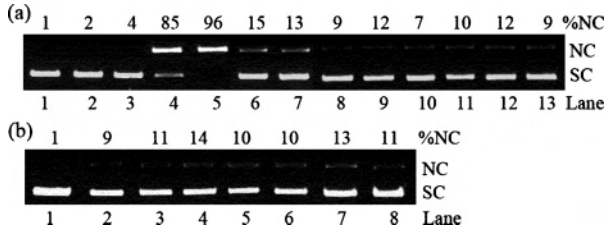

Figure 7. Cleavage of SC pUC19 DNA (0.2 μg, 33.3 μM) by [VO(salmet)(B)] (B = phen, **1**; dpq, **2**; dppz, **3**) and [VO(saltrp)(B)] (B = phen, **4**; dpq, **5**; dppz, **6**) (66.6 μM) in the presence of reducing agents MPA (0.5 mM), glutathione (0.5 mM), and oxidizing agent H_2O_2 (0.5 mM) in 50 mM Tris-HCl/NaCl buffer (pH 7.2) containing 10% DMF under dark reaction conditions: (a) lane 1, DNA control; lane 2, DNA + MPA; lane 3, DNA + glutathione; lane 4, DNA + $[Cu(phen)_2(H_2O)](ClO_4)_2$ + MPA; lane 5, DNA + $[Cu(phen)_2(H_2O)](ClO_4)_2$ + glutathione; lanes 6−11, DNA + complexes **1**−**6** + MPA; lane 12, DNA + **2** + glutathione; lane 13, DNA + **4** + glutathione. (b) Lane 1, DNA control; lane 2, DNA + H_2O_2; lanes 3−8, DNA + complexes **1**−**6** + H_2O_2.

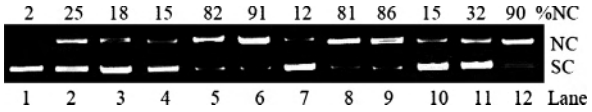

Figure 8. Cleavage of SC pUC19 DNA (0.2 μg, 33.3 μM) by complexes **1**−**6** (33.3 μM) in 50 mM Tris-HCl/NaCl buffer (pH, 7.2) containing 10% DMF on photoirradiation at 365 nm (12 W) for an exposure time of 2 h: lane 1, DNA control; lane 2, DNA + dpq (33.3 μM); lane 3, DNA + dppz (33.3 μM); lanes 4−9, DNA + complexes **1**−**6**; lane 10, DNA + distamycin-A (50 μM); lane 11, DNA + distamycin-A (50 μM) + **2**; lane 12, DNA + distamycin-A (50 μM) + **3**.

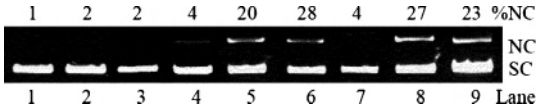

Figure 9. Cleavage of SC pUC19 DNA (33.3 μM) by complexes **1**−**6** in 50 mM Tris-HCl/NaCl buffer (pH, 7.2) containing 10% DMF at red light of λ >750 nm (150 mW) with an exposure time of 2 h: lane 1, DNA control; lane 2, dpq control; lane 3, dppz control; lanes 4−9, DNA + complexes **1**−**6** (66.6 μM).

to be cleavage inactive, while $[Cu(phen)_2]^{2+}$ (5 μM), used as a control, efficiently cleaves DNA in the presence of MPA (Figure 7). The "chemical nuclease" activity of the bis-phen copper(II) complex is due to formation of a reactive copper(I) species that activates molecular oxygen to form a hydroxyl radical and/or copper−oxo species that cleaves DNA by abstraction of the deoxyribose sugar hydrogen atom.[40] A similar mechanistic pathway seems to be unfavorable for the present complexes, showing $V^VO^{3+}/V^{IV}O^{2+}$ and $V^{IV}O^{2+}/V^{III}O^{+}$ redox couples near 0.8 and −1.2 V, respectively, with a potential window of 2.0 V. While the present complexes are inactive "chemical nucleases", oxo-bridged divanadium(III) complexes having 1,10-phenanthroline are known to cleave plasmid DNA by formation of hydroxyl or superoxide radicals.[68] Similarly, bleomycin−vanadyl(IV) and VO(phen)$^{2+}$ complexes oxidatively cleave DNA in the presence of hydrogen peroxide.[47,48] There are few reports on "chemical nuclease" active oxovanadium(IV) complexes used as anticancer agents.[48]

Photonuclease Activity. The photoinduced DNA cleavage activity of the complexes has been studied using SC pUC19 DNA in a medium of Tris-HCl/NaCl buffer on irradiation with monochromatic UV-A light of 365 nm (12 W) and red light of >750 nm (150 mW) (Table 5, Figures 8 and 9). The phen complexes in the absence of any photoactive moiety are a poor cleaver of DNA on exposure to UV-A light. A 33.3 μM solution of the dpq complexes **2** and **5** on irradiation at 365 nm for 2 h shows essentially complete cleavage of SC DNA to its nicked circular (NC) form. The dppz complexes **3** and **6** also display efficient DNA cleavage activity at 365 nm. The photoinduced DNA cleavage activity of the dpq and dppz complexes could be due to the photosensitizing effect of the quinoxaline and phenazine moieties. Control experiments with only SC DNA exposed to 365 nm or the SC DNA in the presence of dpq or dppz complex in dark do not show any DNA cleavage activity. The ligands alone are cleavage inactive under similar reaction conditions. The DNA binding property of the complexes was studied using DNA minor groove binder distamycin-A (Figure 8). Distamycin-A (50 μM) alone shows ∼15% cleavage of SC DNA (33.3 μM) at 365 nm (t = 2 h). Addition of the dpq complexes to SC DNA in the presence of distamycin-A shows significant inhibition in the cleavage activity. The dppz complexes, however, display no apparent inhibition, suggesting minor and major groove binding nature of the dpq and dppz complexes, respectively.[22]

The photoinduced DNA cleavage activity of the complexes in red light was studied using a CW Ar−Kr mixed-gas ion laser with an IR attachment (752.5−799.3 nm) using different complex concentrations (Figure 9). The choice of wavelength is based on the observation of a d−d band of the complexes near 700 nm in the electronic spectra. While the phen complexes are cleavage inactive, the dpq and dppz complexes show significant cleavage of DNA from its SC to NC form at the near-IR wavelength of ∼750 nm. Photoexcitation of the metal complexes seems to be metal assisted and involves the metal-based charge-transfer and d−d bands, resulting in an excited state that generates DNA cleavage active species. Although there are few reports on vanadium(V) complexes showing photocleavage of DNA at UV light, observation of DNA cleavage in red light is unprecedented in the literature.[49−52]

Mechanistic Studies. DNA cleavage reactions were carried out in the presence of different additives to understand the mechanistic pathways involved in the photocleavage reactions (Figure 10). The complexes are cleavage inactive at 365 nm in an argon atmosphere, indicating the necessity of molecular oxygen for cleaving DNA on photoactivation. The DNA cleavage reactions involving $^3O_2$ could proceed via two major mechanistic pathways. The singlet excited electronic state of the complex through efficient intersystem crossing could generate an excited triplet state of the complex that can activate molecular oxygen from its stable triplet ($^3O_2$,$^3\Sigma_g^-$) to the reactive singlet ($^1O_2$,$^1\Delta_g$) state by a type-II process.[9] In an alternate pathway, the excited-state complex could reduce molecular oxygen to generate reactive hydroxyl radical. Addition of singlet oxygen quenchers like sodium azide, TEMP, and DABCO to SC DNA significantly inhibits the photoinduced DNA cleavage activity of the complexes. Hydroxyl radical scavenger like DMSO and catalase has no

(68) Otieno, T.; Bond, M. R.; Mokry, L. M.; Walter, R. B.; Carrano, C. J. *Chem. Commun.* **1996**, 37.

Table 5. Photoinduced SC DNA (0.2 μg, 33.3 μM) Cleavage Data[a]

Sl no.	reaction condition	[complex]: 365 nm [>750 nm]/μM	*t*/h	%NC$_{365\ nm}$ [%NC$_{>750\ nm}$]
1	DNA control		2	2 [2]
2	DNA + [VO(salmet)(dpq)] (**2**) (in dark)	33.3 [66.6]	2	3
3	DNA + [VO(salmet)(phen)] (**1**)	33.3 [66.6]	2	15 [4]
4	DNA + [VO(salmet)(dpq)] (**2**)	33.3 [66.6]	2	82 [20]
5	DNA + [VO(salmet)(dppz)] (**3**)	33.3 [66.6]	2	91 [28]
6	DNA + [VO(saltrp)(phen)] (**4**)	33.3 [66.6]	2	12 [4]
7	DNA + [VO(saltrp)(dpq)] (**5**)	33.3 [66.6]	2	81 [27]
8	DNA + [VO(saltrp)(dppz)] (**6**)	33.3 [66.6]	2	86 [23]

[a] Exposure time, *t*. SC and NC are supercoiled and nicked circular forms of pUC19 DNA. The error in measuring %DNA is ~5%. The absorbance of the complexes at 750 nm is ~0.03 in DMF. Light source: UV light (365 nm, 12 W). [Ar−Kr CW laser (>750 nm, 150 mW)]. Additional data on ligands and vanadyl sulfate (33.3 μM) alone (%NC for 2h photoexposure): dpq, 25%; dppz, 18%; salmet, 8%; saltrp, 9% and $VOSO_4$, 4% at 365 nm.

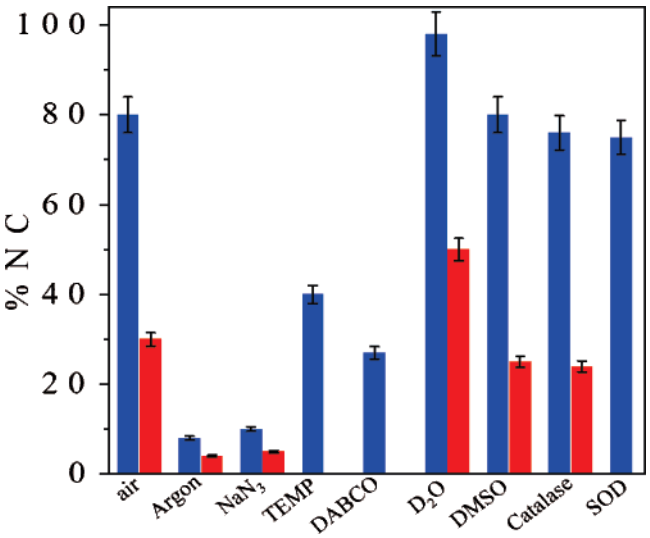

Figure 10. Cleavage of SC pUC19 DNA (33.3 μM) by [VO(salmet)(dpq)] (**2**) in the presence of various additives on irradiation at 365 (blue) and >750 nm (red) for 2 h with a complex concentration of 33.3 and 66.6 μM, respectively, in Tris-HCl buffer containing 10% DMF. The additive concentrations/quantity are as follows: sodium azide (0.5 mM), TEMP (0.5 mM), DABCO (0.5 mM), D_2O (14 μL), DMSO (4 μL), catalase (4 units), and SOD (4 units).

apparent effect on the cleavage activity. The results suggest the involvement of singlet oxygen in the photocleavage reactions in UV-A light of 365 nm. Formation of singlet oxygen is also indicated from the reaction in D_2O, showing enhancement of the cleavage activity due to the longer lifetime of $^1O_2$ in this medium.[69] Bases dpq, dppz, and vanadyl sulfate alone do not show DNA cleavage activity at 365 nm under similar experimental conditions. Control experiments in red light (>750 nm) also show the involvement of singlet oxygen as the reactive species.

Conclusions

We present the first report on the photoinduced DNA cleavage activity of oxovanadium(IV) complexes in the PDT window. The VO^{2+} complexes of *O,N,O*-donor α-amino acid Schiff bases and *N,N*-donor phenanthroline bases as DNA binder cum photosensitizer display efficient DNA binding propensity. The dpq and dppz complexes show photoinduced DNA cleavage activity on photoirradiation at 365 nm and red light of >750 nm by a singlet oxygen pathway. The DNA cleavage observed on photoactivation at a near-IR wavelength is significant. Porphyrin bases including Photofrin are known to cleave DNA on photoirradiation at the Q bands at relatively shorter wavelengths.[1] Photocleavage of DNA at near IR wavelength (>700 nm) is important for PDT applications as the human tissue has greater penetration at longer wavelengths than at 630 nm, the wavelength used for Photofrin activity. Among the macrocyclic organic dyes, lutetium texaphyrin (LUTRIN) is known to cleave DNA on photoirradiation at near-IR wavelength.[1,15] The other significant result is the observation of a wide redox voltage window of ~2.0 V for these oxovanadium(IV) complexes, thus making them to show poor "chemical nuclease" activity. This has relevance to PDT since redox-active iron and copper complexes showing dark toxicity in a cellular medium are unsuitable for PDT applications. The photoinduced DNA cleavage activity of the VO^{2+} complexes of dpq and dppz ligands in red light is unprecedented in the literature. The results are of importance toward designing and developing new oxovanadium(IV) complexes as potential agents for cellular applications in PDT.

Acknowledgment. We thank the Department of Science and Technology, Government of India, for financial support (SR/S1/IC-10/2004) and the CCD diffractometer facility. We also thank the Council of Scientific and Industrial Research, New Delhi, for financial support and a fellowship to A.K.P. We are grateful to the Alexander von Humboldt Foundation, Germany, for an electrochemical system and the Convener, Bioinformatics Center of our Institute, for database search.

Supporting Information Available: Unit cell packing diagrams for complexes **1, 2**, and **4** (Figures S1−S3), electronic spectra (Figures S4, S5), cyclic voltammograms (Figure S6), DNA melting plots (Figure S7), viscosity plots (Figure S8), gel electrophoresis diagrams [photoinduced DNA cleavage activity at 365 nm (Figures S9−S12) and red light (Figures S13−S15)], mass spectra (Figures S16−S21), tables listing of full crystallographic data, atomic coordinates, full list of bond distances and angles, anisotropic thermal parameters, and hydrogen-atom coordinates for complexes **1**·2H_2O, **2**, and **4**·0.5CH_3OH (CIF). This material is available free of charge via the Internet at http://pubs.acs.org.

IC7011793

(69) (a) Khan, A. U. *J. Phys. Chem.* **1976**, *80*, 2219. (b) Merkel, P. B.; Kearns, D. R. *J. Am. Chem. Soc.* **1972**, *94*, 1029.